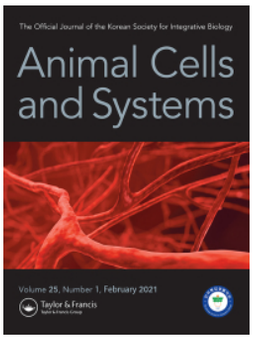

Animal Cells and Systems

ISSN: 1976-8354 (Print) 2151-2485 (Online) Journal homepage: www.tandfonline.com/journals/tacs20

Proteomics and phosphoproteomics of human colorectal cancer cells lacking a specific kinase activity reveal kinase-specific compensatory responses

Bitnara Han, Hyun Ji Lim, Su-Jung Kim, Jaejin Shin, Hyeong Hwan Kim, Kyun-Hwan Kim, Chang-Hoon Nam & Kwang Pyo Kim

To cite this article: Bitnara Han, Hyun Ji Lim, Su-Jung Kim, Jaejin Shin, Hyeong Hwan Kim, Kyun-Hwan Kim, Chang-Hoon Nam & Kwang Pyo Kim (2026) Proteomics and phosphoproteomics of human colorectal cancer cells lacking a specific kinase activity reveal kinase-specific compensatory responses, Animal Cells and Systems, 30:1, 219-234, DOI: 10.1080/19768354.2026.2625524

To link to this article: https://doi.org/10.1080/19768354.2026.2625524

ANIMAL CELLS AND SYSTEMS
2026, VOL. 30, NO. 1, 219–234
https://doi.org/10.1080/19768354.2026.2625524

Proteomics and phosphoproteomics of human colorectal cancer cells lacking a specific kinase activity reveal kinase-specific compensatory responses

Bitnara Han[a]†, Hyun Ji Lim[b,c]†, Su-Jung Kim[a], Jaejin Shin[d], Hyeong Hwan Kim[e], Kyun-Hwan Kim[d], Chang-Hoon Nam[e] and Kwang Pyo Kim[a,b]

[a]Department of Applied Chemistry, Institute of Natural Science, Global Center for Pharmaceutical Ingredient Materials, Kyung Hee University, Yongin, Republic of Korea; [b]Department of Biomedical Science and Technology, Kyung Hee Medical Science Research Institute, Kyung Hee University, Seoul, Republic of Korea; [c]Department of Genetics and Biotechnology, Graduate School, Kyung Hee University, Yongin, Republic of Korea; [d]Department of Precision Medicine, Sungkyunkwan University School of Medicine, Suwon, Republic of Korea; [e]Aging and Immunity Laboratory, Department of New Biology, Daegu Gyeongbuk Institute of Science and Technology, Daegu, Republic of Korea

ABSTRACT

Cell signaling regulates cell proliferation, survival, and migration, and abnormal kinase activity is often implicated in cancer. Although kinases are key targets for anticancer therapy, drug-induced compensatory signaling and pathway rewiring often drive acquired resistance. These compensatory responses enable tumor cells to maintain proliferation and survival, contributing to acquired drug resistance. In this study, we investigated adaptive responses following the knockout of four specific kinase genes, ERK2, PLK1, PIK3CA, and PAK4, using HCT-116, a human colorectal cancer cell line. Using CRISPR–Cas9, we generated individual knockout cell lines and conducted quantitative proteomic and phosphoproteomic profiling using isobaric tagging and tandem mass tag (TMTs) to evaluate alterations in the signaling landscape. Our integrated analysis quantified 7,531 proteins and 10,877 phosphopeptides, revealing kinase-specific patterns of compensatory signaling. ERK2 knockout was associated with activation of MAPK- and PI3K/AKT-related kinases, whereas PIK3CA knockout induced extensive proteomic remodeling and engagement of pro-survival phosphorylation programs, illustrating distinct modes of signaling network rewiring. Integration of kinase–substrate enrichment analysis (KSEA) with global proteomic data revealed that adaptive kinase activity was largely uncoupled from protein abundance and uncovered a synthetic lethal interaction between ERK2 loss and RPS6KB1 inhibition. Collectively, these findings elucidate how targeted kinase loss drives homeostatic signaling networks in cancer cells. By systemically characterizing cellular-level signaling changes and contextualizing them within known kinase pathways, our results provide insights into synthetic lethality and identify potential therapeutic targets to counteract adaptive resistance to kinase inhibitors.

ARTICLE HISTORY
Received 5 November 2025
Revised 31 December 2025
Accepted 26 January 2026

KEYWORDS
Phosphoproteomics; proteomics; signal-rewiring; CRISPR–Cas9; gene editing

Introduction

The number of deaths attributed to colorectal cancer surpassed 0.9 million (Xi and Xu 2021; Siegel et al. 2023). In recent years, targeted kinase inhibitors have emerged as a more effective therapeutic strategy than conventional cytotoxic drugs for colorectal cancer treatment (Xie et al. 2020). By selectively inhibiting oncogenic kinases, these agents provide greater selectivity for cancer cells and significantly minimize side effects compared to traditional therapies. Nevertheless, the development of drug resistance presents a significant challenge to the long-term effectiveness. Drug resistance can be attributed to various factors, including mutations in the target kinases themselves. Secondary mutations or gene amplifications can alter kinase structure or activity, reducing inhibitor binding affinity and diminishing pathway suppression. Additionally,

CONTACT Chang-Hoon Nam chang@dgist.ac.kr; Kwang Pyo Kim kimkp@khu.ac.kr 333 Techno Jungang-daero, Hyeonpung-eup, Dalseong-gun, Daegu 42988, Republic of Korea; 1732 Deogyeong-daero, Giheung-gu, Yongin-si, Gyeonggi-do 17104, Republic of Korea
†These authors contributed equally to this work.

Supplemental data for this article can be accessed online at https://doi.org/10.1080/19768354.2026.2625524.

drug-induced compensatory signaling and pathway rewiring contribute critically to resistance. Cancer cells exhibit substantial signaling plasticity and can activate alternative signaling pathways in response to kinase inhibition, thereby bypassing the blocked pathway and sustaining their proliferation and survival (Rao et al. 2025).

To better understand and overcome these resistance mechanisms, it is essential to study the key kinases that drive colorectal cancer progression. Among these, ERK2 (Mitogen-activated protein kinase 1), PLK1 (Polo-like kinase 1), PIK3CA (Phosphatidylinositol-4,5-bisphosphate 3-kinase catalytic subunit alpha), and PAK4 (p21-activated kinase 4) have emerged as central regulators of oncogenic signaling. ERK2 is a core component of the MAPK pathway and is frequently activated in colorectal tumors, where it promotes cell proliferation and survival. For example, ERK2-mediated phosphorylation of CSN6 (COP9 signalosome subunit 6) stabilizes β-catenin and promotes colorectal tumor development (Fang et al. 2015). Furthermore, TRAPPC4 (Trafficking protein particle complex subunit 4)-dependent regulation of nuclear ERK2 accumulation has been implicated in modulating colorectal cancer cell proliferation and apoptosis (Zhao et al. 2011). PLK1, a crucial mitotic kinase, is often overexpressed in colorectal cancer and is associated with poor prognosis. Preclinical evidence suggests that PLK1 inhibition enhances sensitivity to standard chemotherapy agents, highlighting its therapeutic potential (Yu et al. 2021). PIK3CA, a component of the PI3K/AKT pathway, is among the most commonly mutated oncogenes in colorectal cancer and promotes tumor growth and therapeutic resistance (Wang et al. 2018; Wang et al. 2024). Furthermore, PAK4, a serine/threonine kinase involved in cytoskeletal organization and cell motility, has been implicated in epithelial–mesenchymal transition (EMT) and tumor invasion (Song et al. 2015; Huang et al. 2022). These kinases are frequently mutated or upregulated in colorectal cancer and serve as potential therapeutic targets due to their involvement in diverse hallmarks of cancer.

The CRISPR–Cas9 gene-editing tool, renowned for its high specificity and efficiency, enables precise genetic modifications. Originally identified in prokaryotes as a component of an adaptive immune defense system against exogenous nucleic acids such as plasmids and viruses, the CRISPR–Cas9 system has since been repurposed as a powerful gene-editing tool. Cas9 is guided by a single-guide RNA (sgRNA) to a complementary DNA sequence, where it induces a site-specific double-stranded break, enabling targeted gene knockout. Owing to its precision and scalability for rapid genome-wide screening, CRISPR–Cas9 has emerged as a promising technology in cancer treatment, facilitating gene therapy for specific diseases (Akram et al. 2020; Jiang et al. 2020). In this study, we investigated adaptive signaling responses following the knockout of each of four key kinase genes – ERK2, PLK1, PIK3CA, or PAK4 – using CRISPR–Cas9-mediated gene knockout. These kinases play central roles in major signaling pathways, with ERK2 functioning in the MAPK pathway, PLK1 regulating mitotic progression, PIK3CA acting in the PI3K/AKT pathway, and PAK4 contributing to cytoskeletal dynamics and cell motility (Ogino et al. 2009; Siu et al. 2010; Parascandolo et al. 2024; Park et al. 2024; Gobran et al. 2025). Each of these kinases is frequently mutated or overexpressed in various cancers, highlighting their biological and clinical relevance. Furthermore, by systemically disrupting these kinases, we sought to explore compensatory signaling mechanisms that arise in response to the inhibition of specific kinases (Ortiz-Ruiz et al. 2025). To this end, we extensively profiled the global proteome and phosphoproteome, unveiling signal rewiring induced by kinase depletion. This integrative analysis provides a valuable resource for understanding adaptive responses within cancer signaling networks and reveals significant implications for enhancing therapeutic strategies, offering insights into strategies to overcome compensatory signaling and resistance to kinase-targeted therapies (Han et al. 2025).

Materials and methods

Experimental design and statistical rationale

Four distinct kinase knockout cell lines – ERK2, PLK1, PIK3CA, and PAK4 – were generated from the HCT-116 human colorectal cancer cell line using CRISPR–Cas9 technology and were obtained from ToolGen (Seoul, Korea). These kinases are well established as key regulators of cell proliferation and colorectal cancer pathogenesis, and inhibitors targeting these kinases have shown anticancer activity in preclinical or clinical research (Samuels et al. 2005; Han et al. 2012; Tabusa et al. 2013; Pashirzad et al. 2021). However, kinase

inhibitors are known to exhibit off-target effects that may not result in the anticipated phenotype (Wynn et al. 2011). To circumvent these limitations, gene editing was employed to generate cell lines, in which specific kinases had been knockout. Gene knockout was achieved by introducing guide RNA and Cas9 plasmids into HCT-116 cells through electroporation. Successful knockout clones were selected based on genotyping data. Confirmed knockout cell lines were harvested, digested into peptides, labeled using TMT, and subsequently pooled. From the pooled samples, 5% of peptides were used for global proteome analysis, while the remaining 95% were subjected to phosphopeptide enrichment. For global proteome analysis, peptides were divided into 12 fractions using high-pH fractionation, while enriched phosphopeptides and acetylated peptides were divided into 12 and 6 fractions, respectively, using mid-pH fractionation. All fractions were analyzed using LC-MS/MS (Thermo Fisher Scientific, Massachusetts, USA). Raw mass spectrometry data were processed using Proteome Discoverer version 2.1 (Thermo Fisher Scientific, Massachusetts, USA). Statistical significance of differential peptide expression was measured using Student's *t*-test.

Cell culture and sample preparation

The HCT-116 cell line was obtained from ATCC (Virginia, USA), and both wild-type and genome-edited HCT-116 cells were maintained in McCoy's 5A medium supplemented with 10% fetal bovine serum and 1% penicillin–streptomycin (Welgene, Gyeongsan, Korea) in a humidified atmosphere with 5% CO_2 at 37°C. The cells were harvested and maintained at −80°C until further use. The harvested cells were lysed with a probe sonicator (Branson, Connecticut, USA) in RIPA buffer supplemented with EDTA, a protease inhibitor cocktail (Thermos Fisher Scientific, Massachusetts, USA), and a phosphatase inhibitor (Roche, Basel, Switzerland). The protein concentration of the lysates was determined using the BCA assay, and 400 µg of protein was aliquoted for digestion.

Protein digestion and TMT labeling

In total, 400 µg of protein from each sample was digested using the filter-aided sample preparation method. Proteins were denatured and reduced in SDT buffer (4% SDS in 0.1 M Tris-HCl, pH 7.6, and 0.1 M dithiothreitol) at 37°C and then transferred to a 30 kDa Microcon filter (Merck Millipore, Massachusetts, USA). Protein samples were washed three times with 8 M urea in 0.1 M Tris-HCl (pH 8.5) to remove SDS, followed by alkylation for 30 min with 55 mM iodoacetamide. Following alkylation, the samples were washed three additional times with 8 M urea. Thereafter, the urea buffer was substituted with 100 mM triethylammonium bicarbonate buffer, and proteins were digested with trypsin at an enzyme-to-protein ratio of 1:50 (w/w) by incubation at 37°C for 12 h. The digested peptides were desalted using C18 Micro Spin Columns (Harvard Apparatus, Massachusetts, USA) and dried with a vacuum concentrator (Hanil Scientific Inc., Gimpo, Korea). Peptides were labeled with the 10-plex TMT reagents (Thermo Fisher Scientific, Massachusetts, USA) according to the manufacturer's instructions. Briefly, TMT reagents were dissolved in anhydrous acetonitrile (ACN), added to each peptide sample, vortexed, and incubated at room temperature for 1 h. Each batch contained two biological replicates of the control and four knockout groups, assigned as follows: controls (126, 129N), ERK2 knockout (127N, 129C), PLK1 knockout (127C, 130N), PIK3CA knockout (128N, 130C), PAK4 knockout (128C, 131). Labeling reactions were quenched with 5% hydroxylamine, after which all TMT-labeled peptides were pooled in equal proportions and concentrated using a vacuum concentrator.

Mid-pH fractionation and phosphopeptide enrichment using immobilized-metal affinity chromatography

To separate peptides based on their hydrophobicity, we performed reversed-phase mid-pH fractionation using an XBridge BEH C18 column (4.6 mm × 250 mm, 5 µm; Waters Corp., Massachusetts, USA) on an Agilent 1290 HPLC system (Agilent Technologies, California, USA). The mobile phase composition was as follows: buffer A (10 mM TEAB in water, pH 7.5) and buffer B (10 mM TEAB in 90% ACN, pH 7.5). Peptides were separated over a gradient of 115 min and collected into 12 fractions (gradient: 0/0, 10/5, 20/5, 80/35, 95/70, 105/70, and 115/0; Tmin/% of solvent B). The separated peptides were desalted using Pierce C18 Micro Spin Columns (Thermo Fisher Scientific, Massachusetts, USA) and dried using a vacuum

concentrator. The desalted fractions were then concatenated into six fractions and subjected to phosphopeptide enrichment using Fe^{3+}-immobilized-metal affinity chromatography (IMAC). Briefly, Ni-NTA agarose bead slurry (QIAGEN, Hilden, Germany) was washed with water and incubated with 100 mM EDTA (pH 8.0) for 30 min on an end-over-end rotator. Then, the beads were charged with 10 mM aqueous $FeCl_3$ solution by incubation for 30 min with end-over-end rotation. Peptides from each fraction were reconstituted in IMAC binding/washing buffer (80% ACN, 0.1% formic acid) and incubated with the Fe^{3+}-IMAC beads for 30 min at room temperature. After incubation, the beads were washed twice with IMAC wash buffer, and phosphopeptides were eluted using a 1:1 (v/v) mixture of ACN and 2.5% ammonia in 2 mM phosphate buffer (pH 10) for 1.5 min. Eluted phosphopeptides were immediately acidified to pH 3.5–4.0 with 10% trifluoroacetic acid and desalted using Pierce C18 Spin Columns.

LC-MS/MS analysis for global and phosphoproteomics

Global and phosphopeptide samples were analyzed using an EASY-nLC II coupled to a Q Exactive Hybrid Quadrupole-Orbitrap Mass Spectrometer (Thermo Fisher Scientific, Massachusetts, USA). Peptides were initially loaded onto a trap column (75 μm × 2 cm, C18, 5 μm) for desalting and subsequently separated on a home-made analytical column (75 μm × 100 cm, C18, 3 μm, 300 Å), as previously described (Lee et al. 2014). The analytical column temperature was maintained at 60°C. The mobile phases comprised solvent A (0.1% formic acid in water) and solvent B (0.1% formic acid in 100% ACN). For global proteome analysis, peptides were eluted using the following gradient: 0/2, 3/5, 5/10, 160/40, 165/50, 166/80, 175/80, 176/2, and 200/2 (Tmin/% of solvent B), at a flow rate of 300 nL/min. For phosphoproteomic analysis, the gradient was set as follows: 0/2, 3/5, 110/17, 150/24, 165/35, 166/80, 175/80, 176/2, and 200/2 (Tmin/% of solvent B). Full MS scans were acquired over an m/z range of 400–2000 at a resolution of 70,000 (MS1). The electrospray ionization voltage was set to 2.5 kV, and the capillary temperature was maintained at 250°C. An AGC target for MS1 scans was set to 3e6. Data-dependent acquisition was performed in positive ion mode, selecting the 12 most abundant precursor ions with charge states of 2–5 for MS/MS fragmentation. MS/MS spectra were acquired at a resolution of 35,000, with a fixed first m/z of 100, an AGC target of 2e5, an isolation window of 0.8 m/z, an exclusion duration of 30 s, and a normalized collision energy of 30. For the phosphoproteomic analyses, identical MS/MS acquisition parameters were used.

Database searching and identification of global and phosphoproteomic data

All tandem spectra were converted from the RAW files to mzXML format using msConvert version 3.0.9134. The MS data were then preprocessed using Post-Experiment Monoisotopic Mass Refinement (PE-MMR) to assign accurate precursor masses to the MS/MS data (Shin et al. 2008). The MS/MS spectra were searched against the Uniprot Homo sapiens database (May 2017, 20595 entries) using Proteome Discoverer version 2.1. For both global proteome and phosphoproteome data searches, cysteine carbamidomethylation (+57.021 Da) and lysine and N-terminal TMT 10-plex modification (+229.163 Da) were designated as fixed modifications. Meanwhile, methionine oxidation (+15.995 Da) was designated as a variable modification. For phosphopeptides, serine, threonine, and tyrosine phosphorylation (+79.980 Da) were included as additional variable modifications. Detailed lists of identified proteins and their phosphorylation sites are provided in Supplementary Tables S1 and S2.

Statistical analysis and gene ontology enrichment analysis

Peptide-level TMT reporter ion intensities were normalized using total ion current normalization. Protein abundance was estimated by adding all TMT reporter ion intensities from all fully tryptic peptides from the same protein group. A two-tailed Student's *t*-test was then used to identify differentially expressed proteins (DEPs) and differentially phosphorylated proteins (DPPs). Proteins and phosphopeptides with p values less than 0.05 were considered significant. Gene ontology enrichment analysis was performed for DEPs and DPPs using g:Profiler (https://biit.cs.ut.ee/gprofiler). Lists of genes encoding significant proteins and phosphopeptides were compared against a background consisting of all identified proteins.

Protein–protein network construction and kinase–substrate enrichment analysis

Kinase–substrate enrichment analysis (KSEA) was performed using the KSEA app (https://casecpb.shinyapps.io/ksea/). This approach integrates phosphorylation fold-change data with curated kinase–substrate relationships derived from the PhosphoSitePlus and NetworKIN 3.0 databases to infer kinase activity changes. Protein–protein interaction information for DEPs was collected from the STRING v11.0 public database (Doncheva et al. 2019). Then, kinase–substrate interaction data were visualized using Cytoscape, with node color representing fold changes in protein or phosphorylation abundance and node size reflecting the number of related substrates (Shannon et al. 2003).

XTT cell proliferation assay

Approximately 0.25×10^5 cells per well were seeded into 24-well plates. At 24 and 48 h after seeding, the medium was replaced with fresh medium containing the indicated concentrations of kinase inhibitors (ulixertinib, alpelisib, volasertib, PF-3758309, MK-2206, GW5074, rac-cct 250863, and PF-4708671), all purchased from Selleck Chem (Texas, USA). After 72 h of treatment, XTT and PMS reagents (Welgene, Gyeongsan, Korea) were added directly to the culture medium and incubated at 37°C for 2 h, according to the manufacturer's protocol. Relative cell viability was calculated by a formula (OD value measured at 450 nm − OD value at 690 nm) using a spectrophotometer. All drugs were dissolved in DMSO.

Results

Proteome and phosphoproteome analysis of kinase-knockout cell lines using LC-MS/MS analysis

This study focused on potential compensatory signaling pathways that emerge following the genetic inhibition of specific kinases to investigate potential compensatory signaling pathways at the intracellular protein level. Comparative analysis of four knockout cell lines against the wild-type control (Figures 1 and 2) resulted in the identification of 7,531 proteins and 10,877 phosphopeptides. The comprehensive datasets, including identified proteins and their phosphorylation sites, are available in Supplementary Tables S1 and S2. Volcano plot analyses revealed that the number of identified DEPs and DPPs varied across the cell lines (Figure 3). In the case of DEPs, a range of 45–215 proteins were detected, while for DPPs, 553–769 phosphopeptides were observed in each knockout cell line compared to the wild type (Figures 2A and 3). We then performed principal component analysis (PCA) and hierarchical clustering to identify the most distinct knockout cell line when compared to wild type (Figures 2B and C). As shown in Figure 2, the PIK3CA knockout cell line exhibited the most substantial differences relative to the wild type in both global proteome and phosphoproteome analyses, whereas the PAK4 and PLK1 knockout cell lines showed the least differences in global proteome and phosphoproteome analyses, respectively.

Kinase–substrate enrichment analysis and functional analysis of differentially phosphorylated proteins

To elucidate kinase activity alterations induced by gene-specific deletions, we performed kinase–substrate enrichment analysis (KSEA) using quantitative phosphoproteomics data, followed by gene ontology (GO) enrichment analysis of kinase substrates to characterize kinases exhibiting significant activity changes and delineate their biological implications (Wiredja et al. 2017). In ERK2 knockout cells (Figure 4A), KSEA revealed increased activity of CAMK2A/B/D/G, DAPK3, ROCK1/2, PRKACA, DMPK, PRKCT, MAPK7, PRKG1, AKT1/2, RAF1, PAK1/5, RPS6KA2/3, MARK1/4, ARAF, CHUK, RPS6KB1, PDK1, and IKBKB, indicating enhanced signaling through MAPK and PI3K/AKT cascades (Creighton et al. 2010; Shrestha et al. 2012; Ebi et al. 2013; Liu et al. 2015; Hamadneh et al. 2021; Zhang et al. 2022). Consistently, GO enrichment analysis further revealed significant association with Ras protein signal transduction, mTOR and TGF-β signaling pathways, and cell proliferation-related processes, suggesting compensatory activation of proliferative and growth-promoting pathways upon ERK2 depletion. In contrast, ATM, PLK4, TTK, CDK1/2, NEK2, and AURKA exhibited decreased activity in ERK2-deficient cells. Substrate-related GO analysis of these downregulated kinases revealed

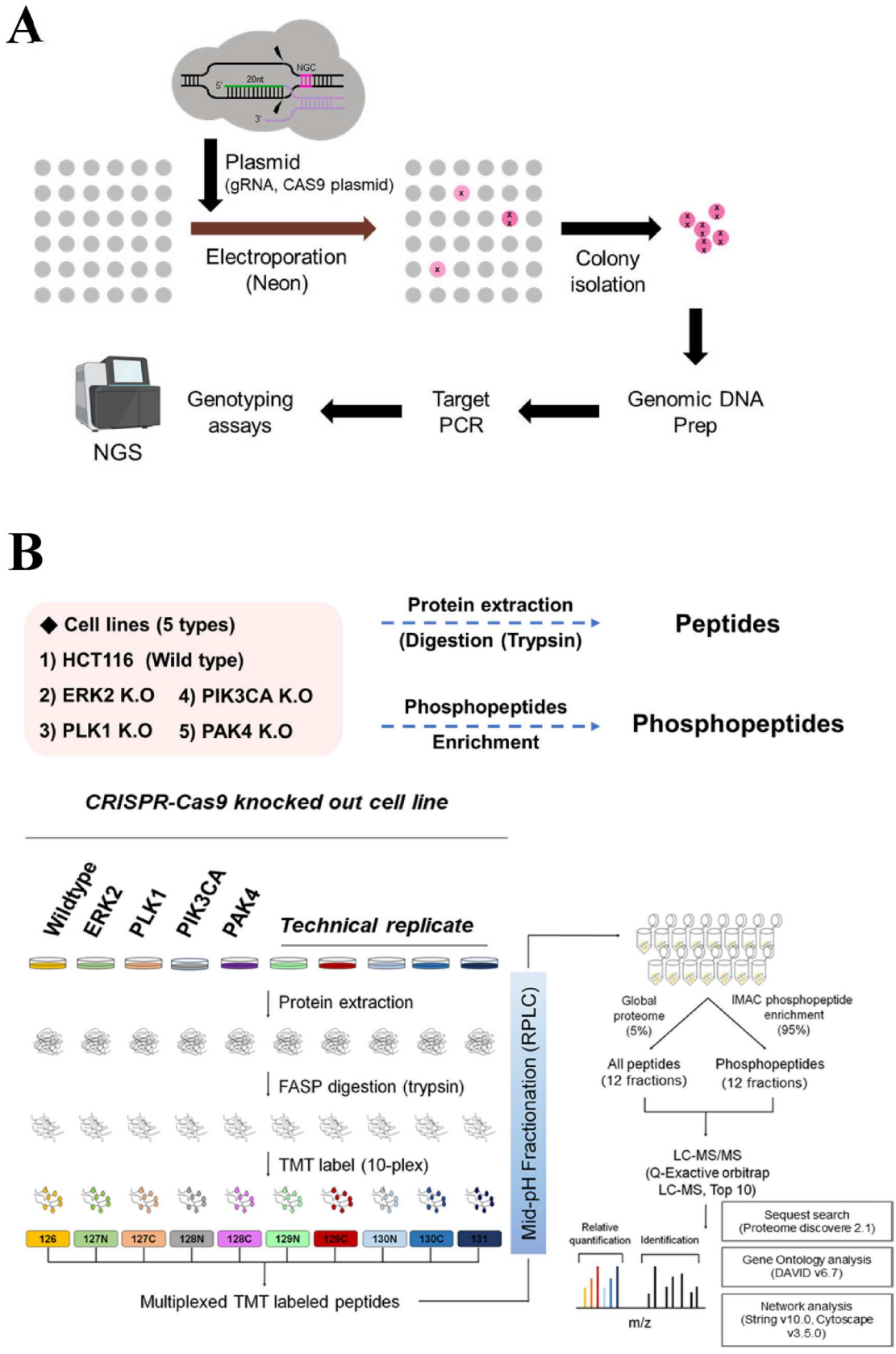

Figure 1. Construction of knockout cell lines using CRISPR–Cas9 and global proteome and phosphoproteome analyses. (A) To knock out four target genes (ERK2, PLK1, PIK3CA, PAK4), guide RNA was prepared for HCT-116 cells, a human colorectal cancer cell line, and then the targets were deleted using Cas9. (B) Scheme of global proteome and phosphoproteome analyses.

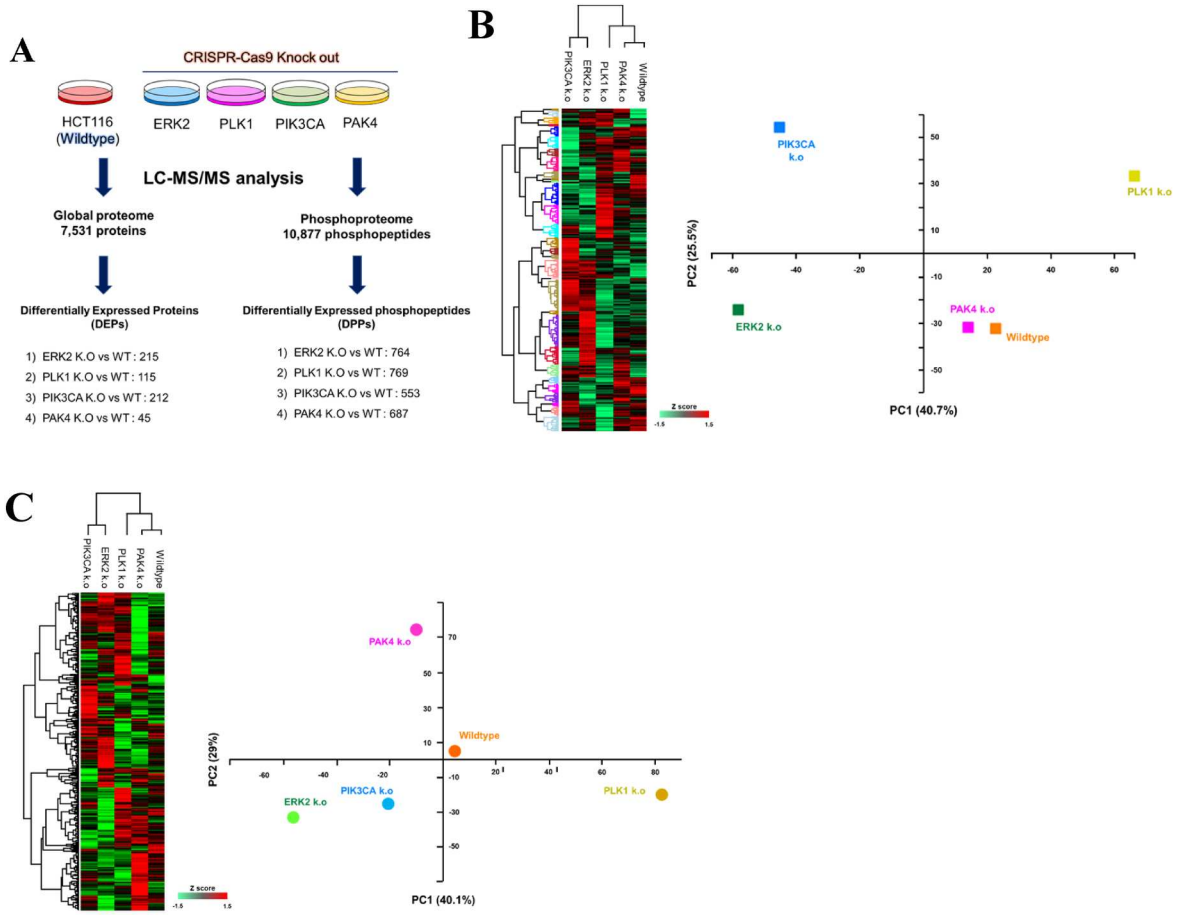

Figure 2. Global proteome and phosphoproteome profiling data for four kinase-knockout cell lines. (A) The number of proteins and phosphopeptides identified by global proteome and phosphoproteome analyses using TMT 10-plex labeling method, including two biological replicates per each knockout cell line, and the number of differential proteins identified following statistical analysis. Hierarchical clustering analysis (HCA) and principal component analysis (PCA) results of (B) global proteome data and (C) phosphoproteome data comparing the four knockout groups and the control group.

enrichment in pathways associated with immune system development, apoptotic processes, cell death, G2/M checkpoint regulation, mitotic cell cycle control, and TP53 phosphorylation-mediated regulation (Turenne and Price 2001; Lin et al. 2002; Falahati and Leitenberg 2007; Guo et al. 2019). Collectively, these results indicate suppression of mitotic checkpoint control and DNA damage–responsive signaling in ERK2-deficient cells.

In PLK1 knockout cells (Figure 4B), AURKA/B, NEK2, TTK, PRKCA/B/D/Z, CDK1, and HIPK2 showed increased activity, consistent with compensatory activation of kinases involved in cell cycle progression, cell division, and Rho GTPase effector signaling (Hogg et al. 1994; Schmidt et al. 2007; Partscht et al. 2023; Lim et al. 2024; Vats et al. 2025). In contrast, AKT1, EIF2AK2, DMPK, MAP2K3/4/6, IKBKB, CAMK2B/D, MAPKAPK2/3/5, PRKACG, CSNK2A1 and PKD1 displayed decreased activity. GO enrichment analysis of substrates corresponding to these downregulated kinases revealed significant associations with apoptotic processes, cell death, and PIP3-mediated AKT signaling, suggesting that PLK1 loss is accompanied by reduced survival and metabolic signaling (Koseoglu et al. 2007; Liu et al. 2020; Hussein et al. 2021; Truebestein et al. 2021; Du et al. 2023).

In PIK3CA knockout cells (Figure 4C), increased activity was observed for GSK3A/B, ROCK1/2, CAMK2B, AKT2/3, MAPK9, PRKCG, and RAF1. Substrate-based GO enrichment analysis revealed significant enrichment for terms related to negative regulation of programmed cell death and negative regulation of apoptotic processes, indicating enhanced pro-survival phosphorylation signaling despite PIK3CA loss (Mure et al. 2010; Tsai and Wei 2010; Fang et al. 2014; Zeng et al. 2014). In contrast, CSNK1A1, NEK2, CLK1, and AURKA exhibited decreased activity, with associated GO terms enriched in cell cycle regulation, cell division, and Rho

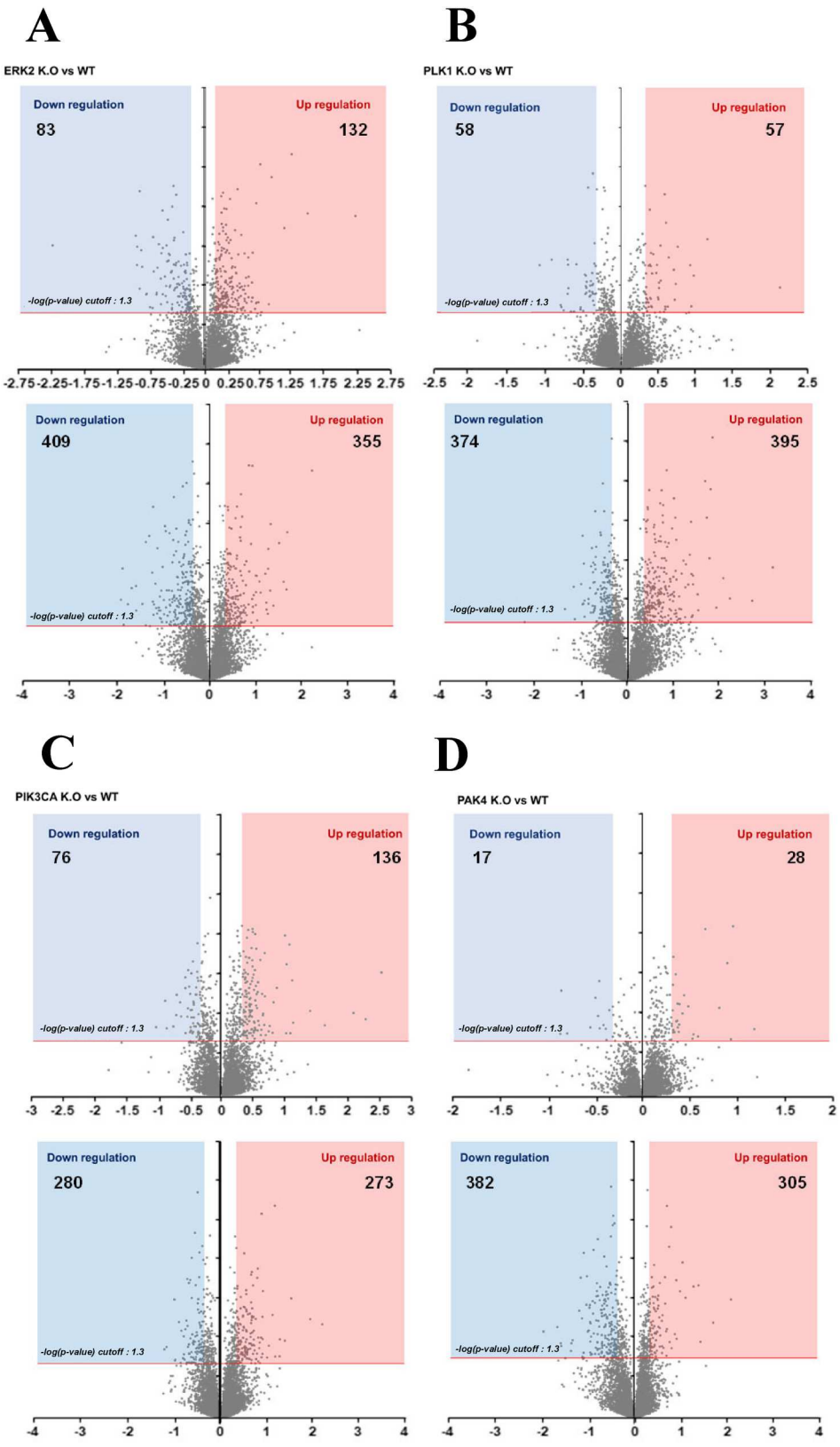

Figure 3. Differential expression analysis of the global proteome and phosphoproteome. Volcano plots showing significant changes in protein expression between the wild-type and each knockout cell line. Differential expression was defined using the criteria $|\log2(\text{fold change})| > 1.3$ and $p < 0.05$ (Student's *t*-test). The horizontal red line indicates the *p*-value threshold. Red and blue boxes denote upregulated and downregulated proteins, respectively. (A) ERK2 knockout, (B) PLK1 knockout, (C) PIK3CA knockout, (D) PAK4 knockout.

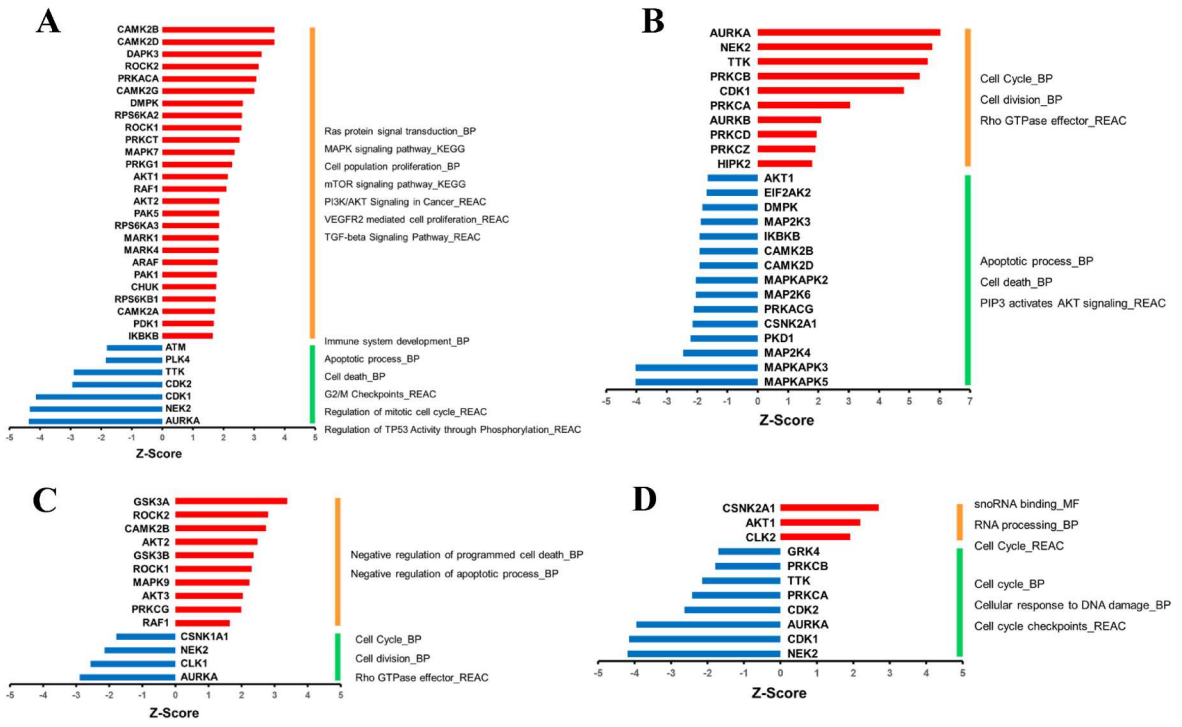

Figure 4. Kinase–substrate enrichment and gene ontology analyses revealing functional differences in kinase activity among knockout cell lines. Kinase–substrate enrichment analysis (KSEA) identifying kinases with significantly altered activity ($|Z\text{-Score}| \geq 2$), integrated with gene ontology-based functional annotations. (A) ERK2 knockout, (B) PLK1 knockout, (C) PIK3CA knockout, (D) PAK4 knockout. BP, biological process; MF, molecular function; REAC, reactome; Wiki, WikiPathways

GTPase effector signaling, implying attenuation of mitotic and cytoskeletal kinase pathways in PIK3CA-deficient cells (Lim et al. 2024).

In PAK4 knockout cells (Figure 4D), CSNK2A1, AKT1, and CLK1 showed increased activity, and GO enrichment of their substrates revealed terms related to cell cycle progression, suggesting compensatory activation of kinases involved in mitotic regulation (Duggal et al. 2018; Chen et al. 2021; Liu 2023). In contrast, GRK4, PRKCA/B, TTK, CDK1/2, AURKA, and NEK2 exhibited decreased activity. Substrate GO terms for these kinases were enriched in cell cycle regulation, cellular responses to DNA damage, and cell cycle checkpoint control, indicating downregulation of checkpoint surveillance and DNA repair–associated signaling pathways (Johnson et al. 2009; Neganova et al. 2011; Ma and Poon 2020; Xu et al. 2020; Qi et al. 2025).

To further investigate the relationship between phosphorylation dynamics and protein abundance, we constructed protein–protein interaction (PPI) networks by integrating KSEA-derived kinase activity changes with global proteomics data (Figure 5A–D). Interestingly, across all knockout cell lines, kinase activity changes inferred from KSEA did not correlate with protein expression levels obtained from the global proteome dataset.

Biological validation of the impact of compensatory signaling pathways on cell proliferation

Based on the results presented above, we hypothesized that blocking the corresponding compensatory or bypass signaling pathways in kinase-deficient cells would synergistically inhibit cell proliferation. In order to verify this, we examined how aberrantly activated kinases and bypassed intracellular signaling pathways affect cell proliferation in each knockout cell line. First, we identified proliferation-related kinases within bypass-activated signaling pathways, inhibited them with kinase inhibitors, and then evaluated the effects of compensatory signaling on cell proliferation.

In ERK2-deficient cells, several kinases implicated in conventional signaling pathways exhibited altered activity. Interestingly, despite ERK2 knockout, phosphorylation of known ERK2 substrates remained, and

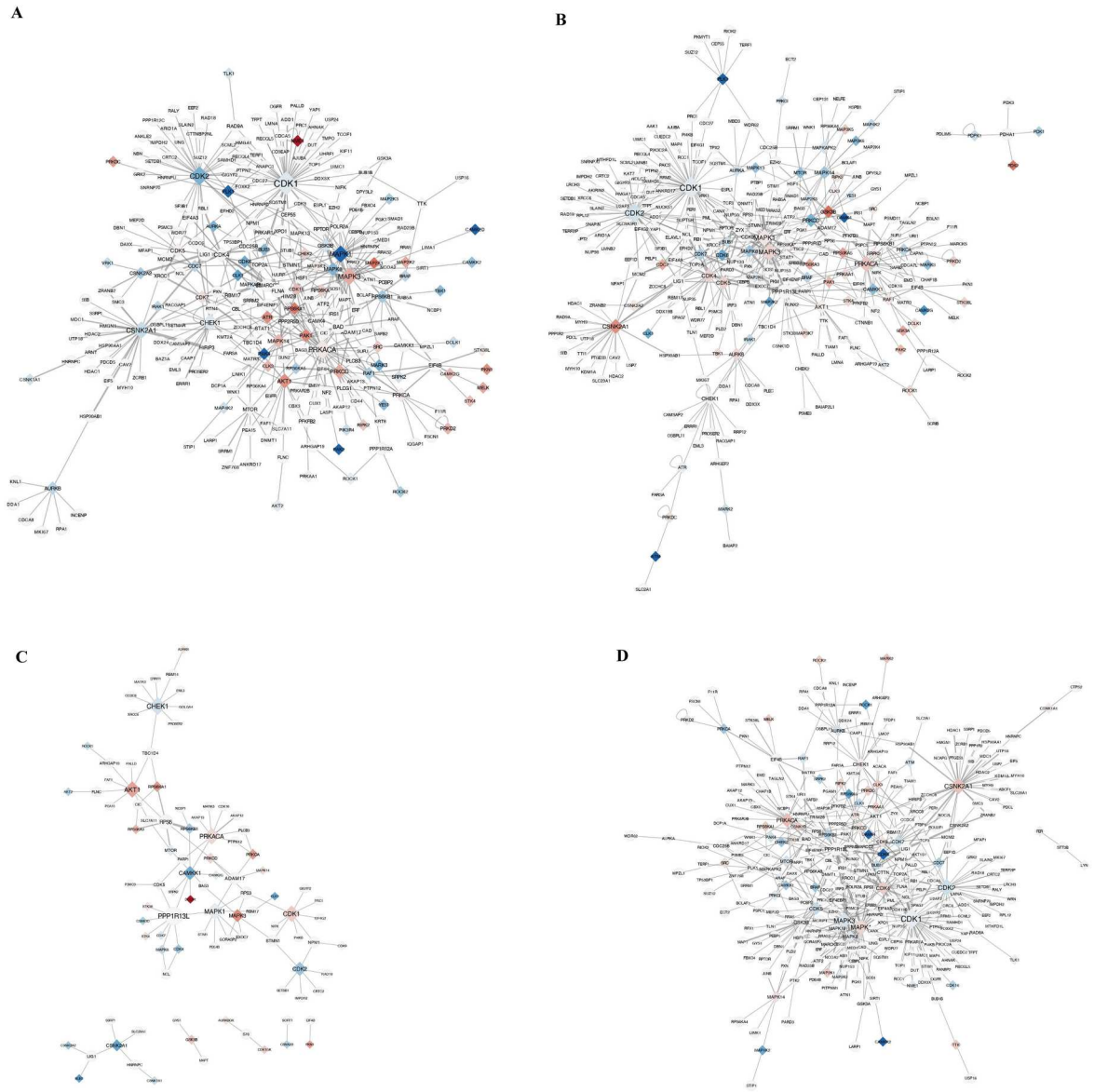

Figure 5. Protein–protein interaction networks integrating kinase–substrate relationships derived from KSEA and DEPs. Protein–protein interaction (PPI) networks were reconstructed by integrating the identified DEPs and KSEA results. Kinases are depicted as rhombuses and their substrates as circles. The size of each rhombus corresponds to the number of associated substrates, and node color indicates relative kinase expression or activity, with red representing upregulated and blue representing downregulated kinase expression; (A) ERK2 knockout, (B) PLK1 knockout, (C) PIK3CA knockout, (D) PAK4 knockout.

cell proliferation was largely maintained (Table 1). Among them, RPS6KB, a member of the mTOR signaling pathway implicated in cell proliferation and motility, was of particular interest (Bahrami et al. 2014). RPS6KB is primarily phosphorylated by mTORC1 kinase but can also be phosphorylated by ERK1 and ERK2, making it a biologically relevant target for functional validation using the XTT assay (Holz 2012; Wang-Bishop et al. 2019).

To determine the effect of ERK2 knockout on maintaining cell proliferation, we treated cells with inhibitors targeting RPS6KB1 (PF-4708671) and AKT1/2 (MK-2206). Three experimental conditions were compared using DMSO as a vehicle control: kinase inhibitor-treated knockout cells, kinase inhibitor-treated wild-type cells, and wild-type cells treated with both kinase inhibitor and knockout gene inhibitor. Notably, PF-4708671 treatment resulted in the most pronounced reduction in cell proliferation in the ERK2 knockout group, whereas minimal effects were observed in the wild-type control groups. Inhibition of AKT1/2 (MK-

Table 1. Comparison of the expression level of ERK2-phosphorylated substrates in the ERK2 knockout cell line

Kinase	Substrate	Phosphorylation site	Kinase log_2FC	Substrate log_2FC	FDR
ERK2	PDE4B	S659	(0.92)	1.35	0.02
	RPS6KB1	S447		0.73	0.02
	NUP153	S338		0.60	0.01
	RBM17	S222		0.58	0.01
	RBM17	T71		0.57	0.01
	PRKAR1A	S83		0.54	0.01
	CEP55	S428		0.53	0.01
	CEBPB	T235		0.53	0.01
	ATF2	T71		0.48	0.01
	POLR2A	S1843		0.48	0.02
	ESPL1	S1126		0.48	0.01
	SOS1	S1210		0.47	0.05
	ERF	S161		0.47	0.02
	ERF	T526		0.47	0.03
	PCBP2	S173		0.47	0.01
	HNRNPK	S284		0.42	0.01
	RPTOR	S696		0.41	0.01
	RAD23B	S160		0.41	0.02
	RRAS2	S186		0.40	0.01
	RAD23B	T155		0.40	0.03
	PGK1	S203		0.37	0.01
	SMAD1	S132		0.34	0.01
	MED1	T1057		0.34	0.01
	MED1	S1156		0.33	0.01

Phosphosite, phosphosite of substrate phosphorylated by ERK2; Kinase FC, log2 value of fold change for kinase in ERK2 knockout cell line; Substrate FC, log2 value of fold change for substrate in ERK2 knockout cell line; Red, log2 negative value.

2206) also reduced proliferation in the ERK2 knockout group, although to a lesser extent. Importantly, neither inhibitor significantly affected cell viability in the wild-type control groups (Figure 6A and B).

In contrast, NEK2, a serine/threonine kinase, was activated in the PLK1 knockout cells. (Figure 4B) NEK2 overexpression promotes colorectal cancer progression via Akt and Wnt signaling pathways and regulation of cell adhesion markers (Neal et al. 2014; Fang and Zhang 2016). However, treatment with a NEK2 inhibitor (rac-cct 250863) showed no statistically significant difference in cell viability between PLK1 knockout and wild-type control groups (Figure 6C).

For PAK4 knockout cells, XTT assays were performed following treatment with an AKT1/2 inhibitor, a key kinase affected by PAK4 knockout. During the assay, however, these cells exhibited excessive sensitivity to DMSO (Supplementary Figure S1), indicating that PAK4 may be essential for maintaining cellular homeostasis and tolerance to external stimuli. These findings illustrate that although compensatory signaling and kinase pathway rewiring are ubiquitously induced by targeted gene knockout, not all upregulated kinases confer effective synthetic lethality when inhibited alongside knockout of the primary target. The persistence

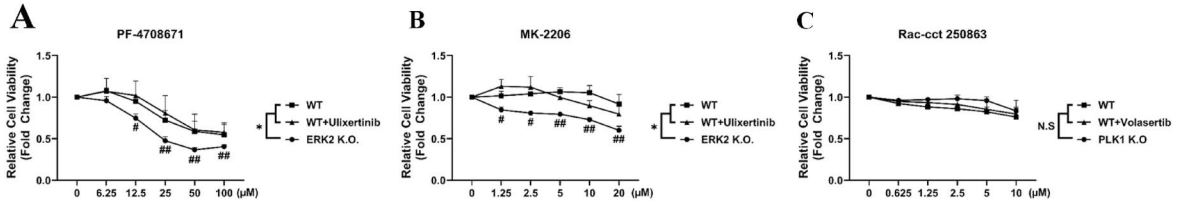

Figure 6. XTT cell proliferation assays evaluating the functional impact of compensatory kinase activation following gene knockout. XTT cell proliferation assays were performed to biologically validate aberrant kinase activities induced by target gene deletion. Cell viability was assessed after 48 h of treatment with kinase inhibitors in ERK2 knockout, PLK1 knockout, and wild-type (HCT-116) cells. (A) PF-470871, (B) MK-2206, and (C) Rac-cct 250863. Proliferation assay results following treatment with the target gene inhibitor and aberrantly activated kinase inhibitor of wild-type cells. Dose ranges were as follows: PF-4708671 (6.25, 12.5, 25, 50, and 100 μM), and MK-2206 (1.25, 2.5, 5, 10, and 20 μM). Rac-cct 250863 (0.625, 1.25, 2.5, 5, and 10 μM). (A, B) Ulixertinib was treated in the order of 50, 100, 200, 400, and 800 nM, and (C) volasertib was treated in the order of 5, 10, 20, 40, and 80 nM. All inhibitors were dissolved in DMSO prior to treatment. Data are presented as mean ± SD. NS, not significant; *$p < 0.05$ vs. knockout group; *p values are from a two-way ANOVA followed by Tukey's test #$p < 0.05$, ##$p < 0.01$ #p values are from a one-way ANOVA followed by Tukey's test. PF-4708671, RPS6KB1 inhibitor; Ulixertinib, ERK2 inhibitor; MK-2206, AKT1/2 inhibitor; Rac-cct 250863, NEK1 inhibitor; Volasertib, PLK1 inhibitor.

of cell proliferation despite dual inhibition highlights the remarkable adaptability and robustness of cancer cell signaling networks. Importantly, these results and our systematic approach demonstrate that targeting certain bypassed pathways, as in the case of ERK2 knockout with RPS6KB1 inhibition, can reveal genotype-specific synthetic lethal interactions. These results underscore the complexity of signaling plasticity and reinforce the importance of functionally validating actionable synthetic lethal pairs to optimize precision cancer therapies.

Discussion

The advent of CRISPR–Cas9 gene-editing technology has revolutionized functional genomics by enabling precise and efficient gene knockout across diverse biological systems (Jinek et al. 2012; Cong et al. 2013; Hong et al. 2024). Leveraging this system, we established kinase-knockout colorectal cancer cell lines in which specific kinases were removed, thereby allowing functional investigation of their roles in diverse cellular processes. Our primary objective was to explore alternative signaling pathways that compensate for the loss of specific kinases by integrating genome editing with global and phosphoproteomic profiling. To this end, we investigated CRISPR–Cas9–engineered HCT-116 cell lines deficient in ERK2, PLK1, PIK3CA, and PAK4, with the aim of characterizing compensatory signaling responses and exploring potential synthetic lethal interactions.

Through quantitative LC-MS/MS–based proteomics, we comprehensively profiled DEPs and DPPs across the four kinase-knockout groups and corresponding controls. This integrated approach revealed that elimination of key intracellular kinases triggers compensatory signaling and induces rewiring of cellular networks. Notably, for most phosphorylation sites, changes in phosphorylation status did not coincide with alterations in the abundance of the corresponding proteins in the global proteome, indicating that extensive signaling adaptation occurred without large-scale alterations in protein levels. Consistent with this observation, phosphorylation of several downstream substrates remained sustained or even enhanced despite the knockout of kinases critical for cell proliferation, implying that kinase regulation under these conditions is largely mediated by post-translational mechanisms and pathway rerouting rather than by differential protein expression. This effect was mediated by other kinases with overlapping functions, highlighting the presence of intricate signaling bypass pathways that enable cancer cells to adapt and survive under targeted kinase inhibition (Cargnello and Roux 2011).

Among the knockout models, the PIK3CA-deficient group exhibited the most prominent alterations in the global proteome, while the ERK2 knockout group had the most pronounced effects on the phosphorylation events. These observations emphasize that different kinases contribute to adaptive signaling through kinase-specific mechanisms. Functional validation through XTT assays further validated the central role of ERK2 in sustaining cell proliferation and demonstrated that inhibition of downstream targets, such as RPS6KB1, can elicit synthetic lethality in ERK2-deficient cells. This finding provides compelling evidence that targeting bypass pathways in combination with kinase inhibition may serve as an effective therapeutic strategy.

As demonstrated in Figure 6, a striking phenomenon was observed, wherein the treatment of ERK2 knockout cells with an RPS6KB1 inhibitor alone produced a greater inhibitory effect on cell proliferation than combined ERK inhibition and RPS6KB1 inhibition in wild-type cells. It is noteworthy that our investigation extended beyond immediate phenotypic effects, encompassing a thorough exploration of the intricate nuances of the interaction in question. Exposure of ERK2 knockout cells to RPS6KB1 inhibitors resulted in a dose-dependent inhibition of cell proliferation. However, this inhibition was not absolute, suggesting the presence of other activated compensatory signaling pathways, as depicted in Figure 4. This suggests a synthetic lethal interaction between ERK2 loss and RPS6KB1 inhibition. Consequently, the substantial decline in cell proliferation observed upon the treatment of ERK2 knockout cells with an RPS6KB1 inhibitor can therefore be attributed to the synthetic lethality of these two genes. Furthermore, we focused on PLK1, a key regulator of the cell cycle and a therapeutic target in colorectal cancer (Francescangeli et al. 2012; Feng et al. 2023). Interestingly, PLK1 knockout unexpectedly led to the activation of NEK2, a cancer-associated kinase. This finding highlights the capacity of cancer cells to rewire kinase networks, whereby loss of one kinase elicits compensatory activation of other kinases to maintain cellular balance.

Collectively, our data demonstrate that loss of individual kinases triggers adaptive signaling responses involving functionally overlapping and compensatory pathways. These findings underscore the inherent

complexity and robustness of intracellular signaling networks in cancer and illustrate the challenges it poses for monotherapy-based treatment strategies (Garraway and Jänne 2012).

Despite the comprehensive proteomic and phosphoproteomic analyses performed in this study, some limitations should be acknowledged. First, this study was conducted in a single colorectal cancer cell line, which may not fully reflect the inter-tumoral heterogeneity. Second, functional validation was restricted to a subset of candidate kinases and bypass pathways, leaving open the possibility that additional compensatory mechanisms remain unexplored. Third, although CRISPR–Cas9 knockout models offer high specificity, they do not entirely mimic the pharmacological inhibition achieved with small-molecule drugs. Future studies should therefore extend to multiple colorectal cancer models, including patient-derived organoids, and integrate *in vivo* validation to better capture tumor complexity and therapeutic response (Shi et al. 2015). Integrating genetic and pharmacological perturbations across diverse models will be essential to comprehensively map synthetic lethal interactions and to identify rational combination therapies to overcome adaptive resistance mechanisms in cancer (Lord and Ashworth 2017; O'Neil et al. 2017).

Authorship contributions

KPK, K-HK, HB conceived and designed this study. HB, K-HK, JS performed the experiment. HB, C-HN, KPK analyzed and interpreted the data. HB, HL, S-JK, HHK, C-HN, KPK wrote the manuscript. All authors approved the final version of the manuscript for publication.

Disclosure statement

No potential conflict of interest was reported by the author(s).

Funding

The research grant of Kyung Hee University in 2024, KHU-202336667 (KPK).

References

Akram F et al. 2020. CRISPR-Cas9, a promising therapeutic tool for cancer therapy: a review. Protein Pept Lett. 27:931–944. https://doi.org/10.2174/0929866527666200407112432

Bahrami BF, Ataie-Kachoie P, Pourgholami MH, Morris DL. 2014. p70 Ribosomal protein S6 kinase (*Rps6kb1*): an update. J Clin Pathol. 67:1019–1025. https://doi.org/10.1136/jclinpath-2014-202560

Cargnello M, Roux PP. 2011. Activation and function of the MAPKs and their substrates, the MAPK-activated protein kinases. Microbiol Mol Biol Rev. 75:50–83. https://doi.org/10.1128/MMBR.00031-10

Chen S et al. 2021. CLK1/SRSF5 pathway induces aberrant exon skipping of METTL14 and Cyclin L2 and promotes growth and metastasis of pancreatic cancer. J Hematol Oncol. 14:60. https://doi.org/10.1186/s13045-021-01072-8

Cong L et al. 2013. Multiplex genome engineering using CRISPR/Cas systems. Science. 339:819–823. https://doi.org/10.1126/science.1231143

Creighton CJ et al. 2010. Proteomic and transcriptomic profiling reveals a link between the PI3K pathway and lower estrogen-receptor (ER) levels and activity in ER+ breast cancer. Breast Cancer Res. 12:R40. https://doi.org/10.1186/bcr2594

Doncheva NT, Morris JH, Gorodkin J, Jensen LJ. 2019. Cytoscape StringApp: network analysis and visualization of proteomics data. J Proteome Res. 18:623–632. https://doi.org/10.1021/acs.jproteome.8b00702

Du HX et al. 2023. Eukaryotic translation initiation factor 2α kinase 2 in pancreatic cancer: an approach towards managing clinical prognosis and molecular immunological characterization. Oncol Lett. 26:478. https://doi.org/10.3892/ol.2023.14066

Duggal S et al. 2018. Defining the Akt1 interactome and its role in regulating the cell cycle. Sci Rep. 8:1303. https://doi.org/10.1038/s41598-018-19689-0

Ebi H et al. 2013. PI3K regulates MEK/ERK signaling in breast cancer via the Rac-GEF, P-Rex1. Proc Natl Acad Sci USA. 110:21124–21129. https://doi.org/10.1073/pnas.1314124110

Falahati R, Leitenberg D. 2007. Changes in the role of the CD45 protein tyrosine phosphatase in regulating Lck tyrosine phosphorylation during thymic development. J Immunol. 178:2056–2064. https://doi.org/10.4049/jimmunol.178.4.2056

Fang L et al. 2015. ERK2-Dependent phosphorylation of CSN6 Is critical in colorectal cancer development. Cancer Cell. 28:183–197. https://doi.org/10.1016/j.ccell.2015.07.004

Fang M, Feng C, Zhao YX, Liu XY. 2014. Camk2b protects neurons from homocysteine-induced apoptosis with the involvement of HIF-1α signal pathway. Int J Clin Exp Med. 7:1659–1668.
Fang YF, Zhang XW. 2016. Targeting NEK2 as a promising therapeutic approach for cancer treatment. Cell Cycle. 15:895–907. https://doi.org/10.1080/15384101.2016.1152430
Feng Y et al. 2023. Inhibition of polo-like kinase 1 (PLK1) triggers cell apoptosis via ROS-caused mitochondrial dysfunction in colorectal carcinoma. J Cancer Res Clin Oncol. 149:6883–6899. https://doi.org/10.1007/s00432-023-04624-2
Francescangeli F et al. 2012. Proliferation state and polo-like kinase1 dependence of tumorigenic colon cancer cells. Stem Cells. 30:1819–1830. https://doi.org/10.1002/stem.1163
Garraway LA, Jänne PA. 2012. Circumventing cancer drug resistance in the era of personalized medicine. Cancer Discov. 2:214–226. https://doi.org/10.1158/2159-8290.CD-12-0012
Gobran M et al. 2025. PLK1 inhibition delays mitotic entry revealing changes to the phosphoproteome of mammalian cells early in division. EMBO J. 44:1891–1920. https://doi.org/10.1038/s44318-025-00400-9
Guo L et al. 2019. Phosphorylation of importin-α1 by CDK1-cyclin B1 controls mitotic spindle assembly. J Cell Sci. 132(18): jcs232314.. https://doi.org/10.1242/jcs.232314
Hamadneh L et al. 2021. PI3K/AKT and MAPK1 molecular changes preceding matrix metallopeptidases overexpression during tamoxifen-resistance development are correlated to poor prognosis in breast cancer patients. Breast Cancer. 28:1358–1366. https://doi.org/10.1007/s12282-021-01277-2
Han D, Lim Y, Lee S, Eyun S-i. 2025. Troponin I – a comprehensive review of its function, structure, evolution, and role in muscle diseases. Animal Cells Syst (Seoul). 29:446–468. https://doi.org/10.1080/19768354.2025.2533821
Han DP et al. 2012. Polo-like kinase 1 is overexpressed in colorectal cancer and participates in the migration and invasion of colorectal cancer cells. Med Sci Monit. 18:Br237–Br246. https://doi.org/10.12659/MSM.882900
Hogg D et al. 1994. Cell cycle dependent regulation of the protein kinase TTK. Oncogene. 9:89–96.
Holz MK. 2012. The role of S6K1 in ER-positive breast cancer. Cell Cycle. 11:3159–3165. https://doi.org/10.4161/cc.21194
Hong T, Bae S-M, Song G, Lim W. 2024. Guide for generating single-cell–derived knockout clones in mammalian cell lines using the CRISPR/Cas9 system. Mol Cells. 47:100087. https://doi.org/10.1016/j.mocell.2024.100087
Huang C et al. 2022. CDK15 promotes colorectal cancer progression via phosphorylating PAK4 and regulating β-catenin/MEK-ERK signaling pathway. Cell Death Differ. 29:14–27. https://doi.org/10.1038/s41418-021-00828-6
Hussein UK et al. 2021. CK2α/CSNK2A1 induces resistance to doxorubicin through SIRT6-mediated activation of the DNA damage repair pathway. Cells. 10(7):1770. https://doi.org/10.3390/cells10071770
Jiang C, Meng L, Yang B, Luo X. 2020. Application of *CRISPR/Cas9* gene editing technique in the study of cancer treatment. Clin Genet. 97:73–88. https://doi.org/10.1111/cge.13589
Jinek M et al. 2012. A programmable dual-RNA-guided DNA endonuclease in adaptive bacterial immunity. Science. 337:816–821. https://doi.org/10.1126/science.1225829
Johnson N et al. 2009. Cdk1 participates in BRCA1-dependent S phase checkpoint control in response to DNA damage. Mol Cell. 35:327–339. https://doi.org/10.1016/j.molcel.2009.06.036
Koseoglu S et al. 2007. AKT1, AKT2 and AKT3-dependent cell survival is cell line-specific and knockdown of all three isoforms selectively induces apoptosis in 20 human tumor cell lines. Cancer Biol Ther. 6(5):755–762. https://doi.org/10.4161/cbt.6.5.3995
Lee H et al. 2014. A fully automated dual-online multifunctional ultrahigh pressure liquid chromatography system for high-throughput proteomics analysis. J Chromatogr A. 1329:83–89. https://doi.org/10.1016/j.chroma.2013.12.084
Lim J et al. 2024. NEK2 phosphorylates RhoGDI1 to promote cell proliferation, migration and invasion through the activation of RhoA and Rac1 in colon cancer cells. Cells. 13(24):2072. https://doi.org/10.3390/cells13242072
Lin HY et al. 2002. Resveratrol induced serine phosphorylation of p53 causes apoptosis in a mutant p53 prostate cancer cell line. J Urol. 168(2):748–755. https://doi.org/10.1016/S0022-5347(05)64739-8
Liu J. 2023. P300 increases CSNK2A1 expression which accelerates colorectal cancer progression through activation of the PI3K-AKT-mTOR axis. Exp Cell Res. 430(1):113694. https://doi.org/10.1016/j.yexcr.2023.113694
Liu Y et al. 2020. Knockdown of IKKβ inhibits tumor development in a leptomeningeal metastasis mouse model and proliferation of lung cancer cells. Cancer Manag Res. 12:6007–6017. https://doi.org/10.2147/CMAR.S252184
Liu Z, Zhu G, Getzenberg RH, Veltri RW. 2015. The Upregulation of PI3K/Akt and MAP Kinase Pathways is Associated with Resistance of Microtubule-Targeting Drugs in Prostate Cancer. J Cell Biochem. 116:1341–1349. https://doi.org/10.1002/jcb.25091
Lord CJ, Ashworth A. 2017. PARP inhibitors: synthetic lethality in the clinic. Science. 355:1152–1158. https://doi.org/10.1126/science.aam7344
Ma HT, Poon RYC. 2020. Aurora kinases and DNA damage response. Mutat Res. 821:111716. https://doi.org/10.1016/j.mrfmmm.2020.111716
Mure H et al. 2010. Akt2 and Akt3 play a pivotal role in malignant gliomas. Neuro Oncol. 12(3):221–232. https://doi.org/10.1093/neuonc/nop026
Neal CP et al. 2014. Overexpression of the Nek2 kinase in colorectal cancer correlates with beta-catenin relocalization and shortened cancer-specific survival. J Surg Oncol. 110(7):828–838. https://doi.org/10.1002/jso.23717
Neganova I et al. 2011. An important role for CDK2 in G1 to S checkpoint activation and DNA damage response in human embryonic stem cells. Stem Cells. 29(4):651–659. https://doi.org/10.1002/stem.620

Ogino S et al. 2009. *PIK3CA* mutation is associated with poor prognosis among patients with curatively resected colon cancer. J Clin Oncol. 27(9):1477–1484. https://doi.org/10.1200/JCO.2008.18.6544
O'Neil NJ, Bailey ML, Hieter P. 2017. Synthetic lethality and cancer. Nat Rev Genet. 18(10):613–623. https://doi.org/10.1038/nrg.2017.47
Ortiz-Ruiz MJ et al. 2025. Mediator kinase inhibitor selectivity and activity in colorectal cancer. ACS Chem Biol. 20(7):1792–1804. https://doi.org/10.1021/acschembio.5c00338
Parascandolo A, Benincasa G, Corcione F, Laukkanen MO. 2024. ERK2 is a promoter of cancer cell growth and migration in colon adenocarcinoma. Antioxidants (Basel). 13(1):119. https://doi.org/10.3390/antiox13010119
Park Y et al. 2024. Integrative transcriptomic profiling uncovers immune and functional responses to bisphenol a across multiple tissues in male mice. Animal Cells Syst (Seoul). 28(1):519–535. https://doi.org/10.1080/19768354.2024.2419473
Partscht P et al. 2023. The HIPK2/CDC14B-MeCP2 axis enhances the spindle assembly checkpoint block by promoting cyclin B translation. Sci Adv. 9(3):eadd6982. https://doi.org/10.1126/sciadv.add6982
Pashirzad M et al. 2021. The therapeutic potential of MAPK/ERK inhibitors in the treatment of colorectal cancer. Curr Cancer Drug Targets. 21(11):932–943. https://doi.org/10.2174/1568009621666211103113339
Qi G et al. 2025. TTK activates ATR through RPA2 phosphorylation to promote olaparib resistance in ovarian cancer. Commun Biol. 8(1):1011. https://doi.org/10.1038/s42003-025-08444-7
Rao J et al. 2025. Multiomics approach identifies key proteins and regulatory pathways in colorectal cancer. J Proteome Res. 24(1):356–367. https://doi.org/10.1021/acs.jproteome.4c00902
Samuels Y et al. 2005. Mutant PIK3CA promotes cell growth and invasion of human cancer cells. Cancer Cell. 7(6):561–573. https://doi.org/10.1016/j.ccr.2005.05.014
Schmidt A, Durgan J, Magalhaes A, Hall A. 2007. Rho GTPases regulate PRK2/PKN2 to control entry into mitosis and exit from cytokinesis. EMBO J. 26(6):1624–1636. https://doi.org/10.1038/sj.emboj.7601637
Shannon P et al. 2003. Cytoscape: a software environment for integrated models of biomolecular interaction networks. Genome Res. 13(11):2498–2504. https://doi.org/10.1101/gr.1239303
Shi J et al. 2015. Discovery of cancer drug targets by CRISPR-Cas9 screening of protein domains. Nat Biotechnol. 33(6):661–667. https://doi.org/10.1038/nbt.3235
Shin B et al. 2008. Postexperiment monoisotopic mass filtering and refinement (PE-MMR) of tandem mass spectrometric data increases accuracy of peptide identification in LC/MS/MS. Mol Cell Proteomics. 7(6):1124–1134. https://doi.org/10.1074/mcp.M700419-MCP200
Shrestha Y et al. 2012. PAK1 is a breast cancer oncogene that coordinately activates MAPK and MET signaling. Oncogene. 31(29):3397–3408. https://doi.org/10.1038/onc.2011.515
Siegel RL et al. 2023. Colorectal cancer statistics, 2023. CA Cancer J Clin. 73(3):233–254. https://doi.org/10.3322/caac.21772
Siu MK et al. 2010. p21-activated kinase 4 regulates ovarian cancer cell proliferation, migration, and invasion and contributes to poor prognosis in patients. Proc Natl Acad Sci USA. 107(43):18622–18627. https://doi.org/10.1073/pnas.0907481107
Song B et al. 2015. P21-activated kinase 1 and 4 were associated with colorectal cancer metastasis and infiltration. J Surg Res. 196(1):130–135. https://doi.org/10.1016/j.jss.2015.02.035
Tabusa H, Brooks T, Massey AJ. 2013. Knockdown of PAK4 or PAK1 inhibits the proliferation of mutant KRAS colon cancer cells independently of RAF/MEK/ERK and PI3K/AKT signaling. Mol Cancer Res. 11(2):109–121. https://doi.org/10.1158/1541-7786.MCR-12-0466
Truebestein L et al. 2021. Structure of autoinhibited Akt1 reveals mechanism of PIP(3)-mediated activation. Proc Natl Acad Sci USA. 118(33):e2101496118. https://doi.org/10.1073/pnas.2101496118
Tsai NP, Wei LN. 2010. Rhoa/ROCK1 signaling regulates stress granule formation and apoptosis. Cell Signal. 22(4):668–675. https://doi.org/10.1016/j.cellsig.2009.12.001
Turenne GA, Price BD. 2001. Glycogen synthase kinase3 beta phosphorylates serine 33 of p53 and activates p53's transcriptional activity. BMC Cell Biol. 2:12. https://doi.org/10.1186/1471-2121-2-12
Vats P et al. 2025. Aurora kinases signaling in cancer: from molecular perception to targeted therapies. Mol Cancer. 24(1):180. https://doi.org/10.1186/s12943-025-02353-3
Wang H, Tang R, Jiang L, Jia Y. 2024. The role of PIK3CA gene mutations in colorectal cancer and the selection of treatment strategies. Front Pharmacol. 15:1494802. https://doi.org/10.3389/fphar.2024.1494802
Wang Q et al. 2018. PIK3CA mutations confer resistance to first-line chemotherapy in colorectal cancer. Cell Death Dis. 9(7):739. https://doi.org/10.1038/s41419-018-0776-6
Wang-Bishop L et al. 2019. Inhibition of AURKA reduces proliferation and survival of gastrointestinal cancer cells with activated KRAS by preventing activation of RPS6KB1. Gastroenterology. 156(3):662–675.e7. https://doi.org/10.1053/j.gastro.2018.10.030
Wiredja DD, Koyuturk M, Chance MR. 2017. The KSEA App: a web-based tool for kinase activity inference from quantitative phosphoproteomics. Bioinformatics. 33(21):3489–3491. https://doi.org/10.1093/bioinformatics/btx415
Wynn ML et al. 2011. Kinase inhibitors can produce off-target effects and activate linked pathways by retroactivity. BMC Syst Biol. 5:156. https://doi.org/10.1186/1752-0509-5-156

Xi Y, Xu P. 2021. Global colorectal cancer burden in 2020 and projections to 2040. Transl Oncol. 14(10):101174. https://doi.org/10.1016/j.tranon.2021.101174

Xie YH, Chen YX, Fang JY. 2020. Comprehensive review of targeted therapy for colorectal cancer. Signal Transduct Target Ther. 5(1):22. https://doi.org/10.1038/s41392-020-0116-z

Xu T et al. 2020. Targeting NEK2 impairs oncogenesis and radioresistance via inhibiting the Wnt1/β-catenin signaling pathway in cervical cancer. J Exp Clin Cancer Res. 39(1):183. https://doi.org/10.1186/s13046-020-01659-y

Yu Z et al. 2021. Inhibition of the PLK1-coupled cell cycle machinery overcomes resistance to oxaliplatin in colorectal cancer. Adv Sci (Weinh). 8(23):e2100759. https://doi.org/10.1002/advs.202100759

Zeng J et al. 2014. GSK3β overexpression indicates poor prognosis and its inhibition reduces cell proliferation and survival of non-small cell lung cancer cells. PLoS One. 9(3):e91231. https://doi.org/10.1371/journal.pone.0091231

Zhang Z, Richmond A, Yan C. 2022. Immunomodulatory properties of PI3K/AKT/mTOR and MAPK/MEK/ERK inhibition augment response to immune checkpoint blockade in melanoma and triple-negative breast cancer. Int J Mol Sci. 23(13):7353. https://doi.org/10.3390/ijms23137353

Zhao SL et al. 2011. TRAPPC4-ERK2 interaction activates ERK1/2, modulates its nuclear localization and regulates proliferation and apoptosis of colorectal cancer cells. PLoS One. 6(8):e23262. https://doi.org/10.1371/journal.pone.0023262